Universidade de Aveiro

Departamento de Física

Ano 2020

Pedro Miguel Negreiros Capelas

Estudo e visualização da densidade de estados conjunta do modelo de Ising por métodos Monte-Carlo

Nº Mec.: 89139

Relatório de Projeto

Mestrado Integrado em Engenharia Física

2019/2020

Universidade de Aveiro

Departamento de Física

Ano 2020

Pedro Miguel Negreiros Capelas

Study and visualization of the Joint Density of States methods of the Ising model by Monte-Carlo methods

Nº Mec.: 89139

palavras-chave

Densidade de estados conjunta, método Wang-Landau, Amostragem de caminho aleatório, método Hüller-Pleimling, Monte-Carlo, Modelo de Ising.

resumo

Este trabalho foca-se no estudo do modelo de Ising bi-dimensional numa rede quadrada finita e, em mais detalhe, no cálculo e visualização da sua Densidade de Estados Conjunta utilizando três diferentes métodos baseados em Monte-Carlo: o método de Hüller-Pleimling, Amostragem de Caminho Aleatório e, por fim, o método de Wang-Landau. Para o modelo de Ising com dimensão linear L igual a 4 todos os métodos foram capazes de criar uma Densidade de Estados Conjunta completa, onde a Amostragem de Caminho Aleatório teve o erro relativo mais baixo. Para L igual a 8, o único método que cria uma Densidade de Estados Conjunta completa é o método de Wang-Landau.

keywords Joint Density of States, Wang-Landau method, Random Path Sampling, Hüller-Pleimling method, Monte-Carlo, Ising Model.

abstract This work focuses on the study of the two-dimensional finite square-lattice Ising Model and, in more detail, the calculation and visualization of its Joint Density of States (JDoS) using three different Monte-Carlo based methods: the Hüller-Pleimling method, Random Path Sampling and, lastly, the Wang-Landau method. For the Ising model with linear system size L equal to 4, every studied method is able of creating a complete Joint Density of States, where the Random Path Sampling had the lowest relative error. For L equal to 8, the only method that creates a complete Joint Density of States is the Wang-Landau method.

Contents

Chapter 1

Introduction

Ferromagnetism is, generally, a term that is given to any material that exhibits a spontaneous magnetization, that is, a resulting magnetic moment in the absence of any external magnetic field [1]. One of the most important and defining features of these materials is the fact that they can only sustain this behaviour below a certain temperature. It is typical for the transition from a ferromagnetic to a paramagnetic behaviour to occur abruptly in a very well-defined temperature, normally named critical temperature (T_C). In this specific case the critical temperature is named Curie Temperature.

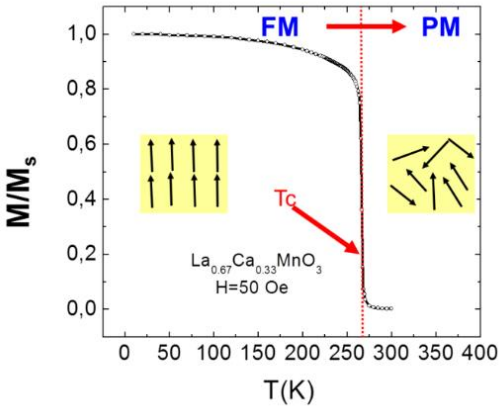

Figure 1 – Magnetization graph for $La_{0.67}Ca_{0.33}MnO_3$ as a function of temperature [2].

The search for more and better ferromagnets has grown over the last couple of decades because of their valuable applications that range from data storage to energy conversion to spintronics. Very few elements can show localized moments while in solid state and even fewer can be used in real world applications. One of the deciding factors that makes this number so low is that the range of temperatures used in real life applications is between -50 ºC and 120 ºC demanding the critical temperatures to be relatively high [3].

The search of a new ferromagnetic material usually proceeds by experimental trial and error after an analysis of a list of potential candidates. To create this list most of the

materials are chosen through chemical intuition, that is, what behaviour should be expected from them. However, exceptions in chemical tendencies happen frequently, slowing down the search for these materials.

In the last two decades, a completely different process with the objective of finding new ferromagnets has been created: the use of computation and numerical methods to create accurate simulations of real-world materials [4]. These computational methods have developed over the years to a degree where their impact is evident. In the last few years, several ferromagnets like Co_2MnTi and $In_2Mn_2O_7$ have been discovered with the help of these tools [3], [5].

Chapter 2

Ising Model

First introduced in 1920 by Lenz, the Ising model is a theoretical model capable of clearly reproducing the phase transition from ferromagnetic to paramagnetic. It consists of spins (of values +1 or -1) that can only be in the sites of a lattice whose interactions between nearest neighbours are considered dominant and periodic boundary conditions (PBC) are used.

It was discovered by Ernst Ising, Lenz's student, that the one-dimensional model could not represent the transition, since it only happened at T = 0 K. However, shortly after, Peierls showed explicitly that in a two-dimensional system there is a well-defined phase transition. In 1944, Lars Onsager solved analytically the two-dimensional square lattice Ising model.

For a long time, the Ising model was seen as a mere simplification of a real-world magnet, one that showed important features of a cooperative system but lacked correspondence to specific materials. However, in the 1950's, with the rise in availability of rare earth elements, the interest in finding new magnets rose too. Soon after, it was discovered that the Ising model was a good approximation of some of those new magnets [6].

This method can show a well-defined non-trivial phase transition while having an analytic solution. This situation gives the unusual possibility of understanding exactly how the system behaves, contrarily to most physical systems [7].

In this study we will only study the two-dimensional square lattice Ising model. This system's Hamiltonian, **H,** is given by

$$\mathbf{H} = -\frac{1}{2}\sum_{<i,j>}\left(J\, S_i \cdot S_j\right) - MH \tag{2.1}$$

where J is the exchange factor, S_i and S_j are spins from the nearest neighbours, H is the applied magnetic field and M is the total magnetization of the system. We will evaluate the

case where there is no applied magnetic field. The exchange factor defines how each spin interacts with its neighbours: if $J > 0$ the interaction will be ferromagnetic, if $J < 0$ the interaction will be antiferromagnetic and, lastly, if $J = 0$ there will be no interaction. For the sake of simplicity, as we want to study a ferromagnetic behaviour, we will define this value as being 1. With everything settled, the Hamiltonian of this system is given by

$$\mathbf{H} = -\frac{1}{2}\sum_{<i,j>}\left(S_i \cdot S_j\right). \tag{2.2}$$

For the square-lattice Ising model with L^2 spins, the total magnetization is given by the sum of every spin in the system,

$$M = \sum_{i=1}^{L^2} S_i\,, \tag{2.3}$$

while the energy is given by the Hamiltonian.

The number of possible configurations for a system with L^2 spins can be calculated by multiplying every spin in the system by the number of possible values it can have (in this case, this number is 2, +1 and -1). As an example, for a small system with 4 spins in total, there are 2^4 possible configurations.

A possible method capable of calculating the thermodynamic properties for this model, like the estimate of T_C and the dependence of the spontaneous magnetization with temperature, is through calculations using the Joint Density of States.

2.1 Joint Density of States

The Joint Density of States (JDoS) is a multi-variable (e.g. energy and magnetization) function that describes the system's microstate distribution in the phase space. In the case of the Ising model, it is represented as $g(E, M)$ and, with it, we can calculate thermodynamic properties like the partition function and Helmholtz free energy, both temperature dependent. It contains much more information than the one variable-energy density of states [8]. The hardest information to obtain from this function is the degeneracy **Ω**: how many different microstates have the same energy-magnetization pair.

Table 1 represents the JDoS of a square-lattice Ising model with L = 2. There are energy-magnetization pairs that only appear in one configuration and that is the case for configurations where every spin is up or down, regardless of the system's size.

Table 1 – JDoS for a simple square Ising model with a total of 4 spins.

M	**E/*J***	**Ω**
4	-8	1
2	0	4
0	0	4
	8	2
-2	0	4
-4	-8	1

To calculate the JDoS of a system, ideally, we need to observe every possible microstate. The fundamental problem is that, for a small system with L = 8, we have 1.84×10^{19} possible microstates. With that said, the probability of configurations with every spin up or down being observed is $2^{-64} \approx 5.4 \times 10^{-20}$, which is impossible to brute force with modern processing power.

To help visualize what the JDoS really is, figure 2 shows it for a square-lattice Ising model with L = 4 from two different angles. As shown, the visualization of the JDoS can be quite hard since some of its values are orders of magnitude larger than others. As a result, we will be showing, when practical, the base 10 logarithm of the JDoS instead.

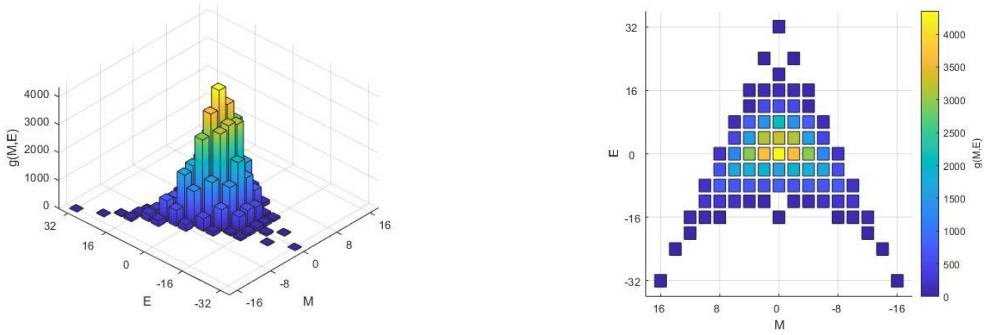

Figure 2 – Exact JDoS for a square-lattice system with a total of 16 spins (L=4).

As explained previously, with the JDoS in hand, we can calculate the equilibrium thermodynamic properties of the system, having access to both the partition function and the free energy. Being a relatively old idea, the use of numerical methods as a solution to complex problems, like calculating the JDoS, has been gaining strength due to the evolution of the processing power present in modern computers. In addition, new methods have been developed to take advantage of parallelization, since it is one of the best ways to reduce computing time.

In this work, three fundamentally different Monte-Carlo based methods to estimate the JDoS of the 2D Ising model will be explored: the Hüller-Pleimling method, Random Path Sampling and, lastly, the Wang-Landau method.

Chapter 3

Monte-Carlo based methods for JDoS calculation

Monte-Carlo is, generally, a term given to any method that uses (and is dependent on) random numbers to obtain numerical results. Two different random number sequences will inevitably result in different values that are related, within a certain statistical error [9]. These kinds of methods can be used in problems that can be discretized. As a starting point, it is important to gain some intuition by observing what happens when we try to explore the energy-magnetization phase space without any bias or criteria, that is, if we do a random walk through phase space.

In a random sampling, every configuration is independent from each other making local energy updates (these will be explained later in this chapter) impossible. To calculate the energy of a completely new configuration, the function "function_Energy_Ising_2D_SS" was used.

In the MATLAB code below, the first part of the function is shown where the nearest neighbours are calculated. This is done with the help of a different function "function_NN_list_2D_SS". This step is fundamental because it allows us to make all kinds of energy calculations.

```
function U = function_Energy_Ising_2D_SS(L,S_vector)

nnxpos = nan(L^2,1);
nnxneg = nan(L^2,1);
nnypos = nan(L^2,1);
nnyneg = nan(L^2,1);

for i = 1:L
    for j = 1:L

       [nnxpos(j+(i-1)*L),nnxneg(j+(i-1)*L),nnypos(j+(i-
       1)*L),nnyneg(j+(i-1)*L)] = function_NN_list_2D_SS(L,i,j);

    end
end
```

The last part will effectively calculate the energy of the configuration based on the Hamiltonian.

```
E = 0;
for i = 1:L
    for j = 1:L
       E = E - 1/2*S_vector(j+(i-1)*L,1)*(S_vector(nnxpos(j+(i-
       1)*L))+S_vector(nnxneg(j+(i-1)*L))+S_vector(nnypos(j+(i-
       1)*L))+S_vector(nnyneg(j+(i-1)*L)));
    end
end
```

As we will see later, every method studied in this work (except random sampling) takes advantage of local energy updates: instead of calculating the Hamiltonian for every spin present in a certain configuration, we calculate the change that results from a flipped spin and we readjust the energy of the original configuration. These local energy updates can be used when a new configuration is related by a flipped spin to a previous configuration (to which we have its energy) and can save a lot of computing time. A local energy update is shown in the next grey box.

```
S_vector(SFV(q-1)) = -1;

dE = - S_vector(SFV(q-1)) .* ( ...
    S_vector(nnxpos((SFV(q-1)))) + ...
    S_vector(nnxneg((SFV(q-1)))) + ...
    S_vector(nnypos((SFV(q-1)))) + ...
    S_vector(nnyneg((SFV(q-1)))));

E = E - 2*dE;
```

One other important concept that must be presented is that of the histogram. Represented by $H(E, M)$, the histogram is, essentially, the building foundation by which we can calculate the JDoS of a system. Different methods have different approaches on how to build their histogram but, generally, it works by adding the value 1 every time a specific microstate is visited.

3.1 Random Sampling

Considering, firstly, a system with L = 4 spins, and exploring 1E6 random configurations, we end up, as expected, with a fully explored phase space (as seen in figure 3). That happens because the number of random configurations explored is larger than the number of possible configurations. The JDoS, in this case, is proportional to the created histogram, and the normalization can be done by dividing the entire histogram by its value that represents the all-up or all-down states.

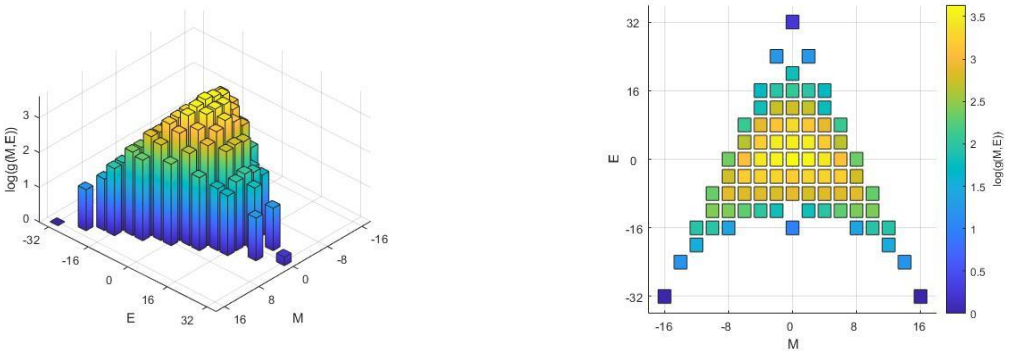

Figure 3 – Logarithm of the normalized JDoS for the random sampling (L = 4).

The construction of the histogram for L = 4 is shown in http://sweet.ua.pt/pedromncapelas/RS14.avi and http://sweet.ua.pt/pedromncapelas/RS24.avi.

Starting with the random sampling, every method will have a grey box where a sample of pseudocode will be presented.

```
Define constants (system size, maximum energy, …)
Calculate Magnetization list
Calculate Energy list
Histogram = 0
for number of repetitions
    Random spin configuration
    Magnetization calculation
    Energy calculation
    Histogram update
end for
JDOS=Histogram/(Value of histogram representing all up configuration)
```

In the first place, 5 constants are defined: the size of the system, the number of nearest neighbours, two vectors that contains every magnetization and energy value and, finally, a matrix that represents the histogram. Following this, a loop is created where, for each

iteration, a random configuration is generated, its energy and magnetization are calculated and, finally, the histogram is updated (by adding 1 to the magnetization-energy pair). The last step is where we turn the histogram into the JDoS by normalizing it. The normalization is done using the fact that we should only observe one configuration with the highest magnetization value: all-up. This way, if we divide the histogram by the value in the histogram that corresponds to the configuration where all spins are up, then we should get an estimate of the JDoS.

For a bigger system with L = 8, we reach the aforementioned situation where the number of configurations is much larger than the number of configurations calculated, not resulting in a fully explored JDoS (figure 4).

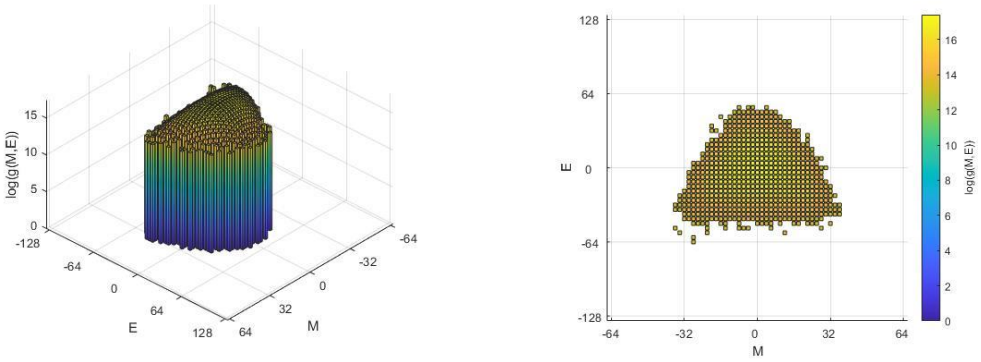

Figure 4 – Logarithm of the normalized JDoS estimate for a square-lattice Ising model with L = 8.

The construction of the histogram for L = 8 is show in http://sweet.ua.pt/pedromncapelas/RS18.avi and http://sweet.ua.pt/pedromncapelas/RS28.avi.

3.2 Hüller-Pleimling Method

The Hüller-Pleimling method, introduced in 2002 [10], seeks to explore the Energy-Magnetization phase space by assessing the rates of the tries associated with the transition between states. The method works by starting with a random microstate, doing random spin flips, and observing how often these microstate transitions occur. To achieve this, three values are defined: Z_{ij} representing the number of times the transition between the microstate i and j was observed, Z_i denominating de number of times the state i was observed and T_{ij} resulting of the division of the first quantity by the second, denominated by transition rate.

A criterion is defined by which each spin flip is accepted (or rejected) and it is given by

$$p(i \rightarrow j) = \begin{cases} 1 \; if \; T_{ij} < T_{ji} \\ \dfrac{T_{ji}}{T_{ij}} \quad else \end{cases}, \tag{3.1}$$

where $p(i \rightarrow j)$ is the probability of the spin flip being accepted. In the end of the algorithm, after the JDoS is created, the probability of visiting any magnetization-energy pair is equal, irrespective of its degeneracy [10].

Every configuration is correlated to the previous configuration by a spin flip, enabling the use of local energy updates. Figure 5 shows the JDoS for a system with L = 4 and 1E6 spin flips.

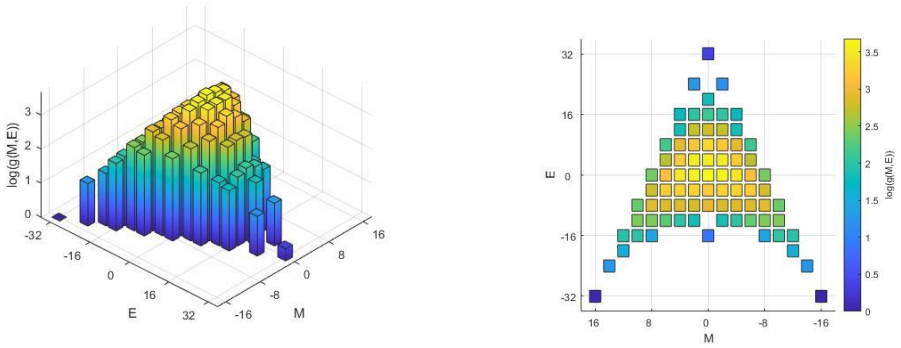

Figure 5 - Logarithm of the normalized JDoS for the Hüller-Pleimling method (L = 4).

The construction of the histogram for L = 4 is show in http://sweet.ua.pt/pedromncapelas/HP14.avi and http://sweet.ua.pt/pedromncapelas/HP24.avi. As we can see, for a small system, every possible microstate is visited, allowing a complete picture of the phase space. However, as we can see for figure 6, for a slightly bigger system with L = 8 and the same 1E6 spin flips, the method struggles to visit most of the possible microstates, getting stuck in the energy-magnetization pairs with the highest degeneracy.

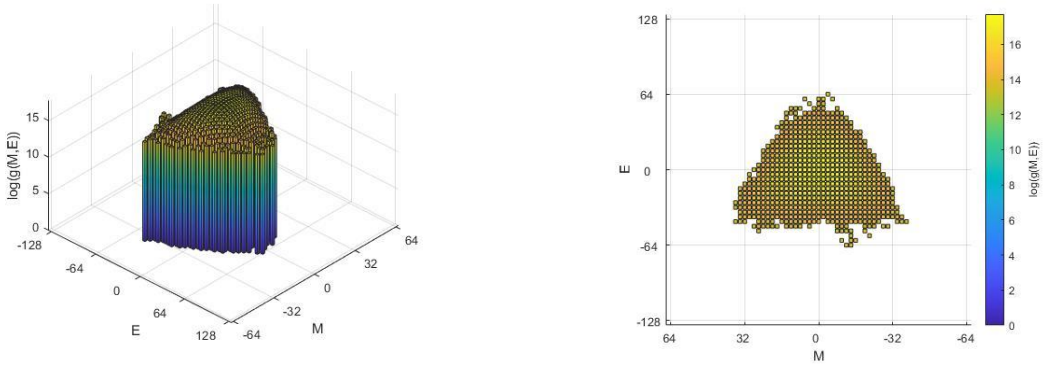

Figure 6 - Logarithm of the incomplete normalized JDoS for the Hüller-Pleimling method (L = 8).

The construction of the histogram for L = 8 is show in http://sweet.ua.pt/pedromncapelas/HP18.avi and http://sweet.ua.pt/pedromncapelas/HP28.avi. In the next grey box a sample of pseudocode is written where it is shown the structure of the Hüller-Pleimling method. Note that both Z_{ij} and Z_i updates are not the same in the *if* and *else* loops.

```
Original configuration
Magnetization and Energy calculation
for number of spin flips
      Spin flip
      Local energy update
      Magnetization calculation
      Direct and Inverse transition rate calculation
      if  spin flip is accepted
            Histogram update
            Zij and Zj update
            New state becomes the Old state
      else
            Spin flip rejected
            Zij and Zi update
            Old state remains unchanged
      end else
      end if
end for
```

3.3 Random Path Sampling

Firstly introduced in 2014 [11], Random Path Sampling (RPS) is a Monte-Carlo based method that, by construction, estimates the JDoS while having a flat magnetization histogram. This method works by starting in the configuration with every spin up and rotating a random spin (which was not already flipped downwards) in each iteration until every spin is flipped downwards. This way, in each RPS sweep, we visit every magnetization value once, resulting in the previously mentioned flat magnetization histogram. To help visualize how the procedure truly works, it is pictured in figure 7. One defining feature of this method is that each configuration is dependent on the last visited configuration (with the exception of the first configuration representing the all up state) enabling the use of local energy updates, which reduces the energy calculation time tremendously.

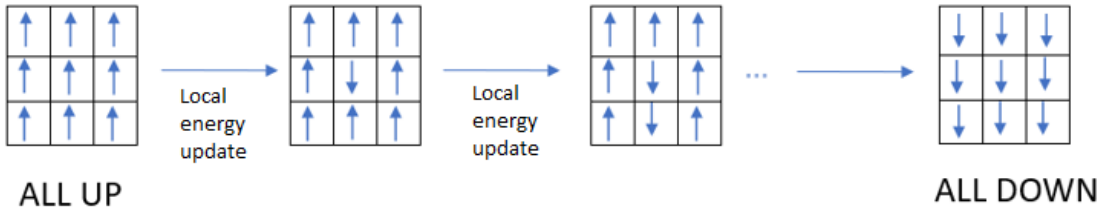

Figure 7 – Procedure scheme for the Random Path Sampling.

To further help in the understanding of this method, figure 8 displays the internal probabilities for L = 2, for each RPS iteration.

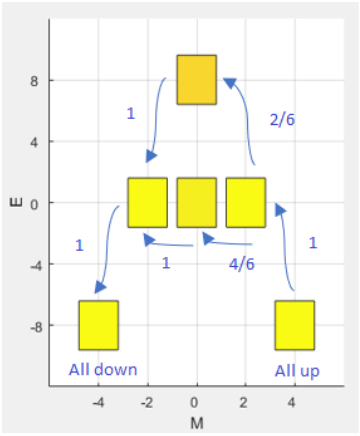

Figure 8 – Internal probabilities for the RPS method for a system with L = 2.

The only non-trivial probability is that of the transition from M = 2 to M = 0 where there are two possible energy values. We can easily search what configurations have those energy values, by trial and error, due to the small size of the system. We reach the conclusion that 2 configurations have an energy value of 8 while 4 configurations have an energy value of 0, rendering the probabilities shown in figure 6. For bigger systems, using trial and error becomes infeasible just by observing that the number of configurations scales exponentially with 2^{L^2}. One relevant fact is that the number of configurations visited, for an even L value, for a given number of RPS sweeps is given by

$$n_C = n_{RPSs} \times M_{values}(L) = n_{RPSs} \times (L^2 + 1) \tag{3.1}$$

where n_{RPSs} is the number of RPS sweeps and $M_{values}(L)$ is the number of magnetization values possible. The last is dependent on the size of the system and is given by $L^2 + 1$. So, although we do the same number of sweeps, the actual number of configurations visited is larger.

Beginning at a system with L = 4 and doing 1E6 RPS sweeps will, as both previous methods, give us a fully explored phase space. The complete histogram for 1E6 sweep is shown in figure 9.

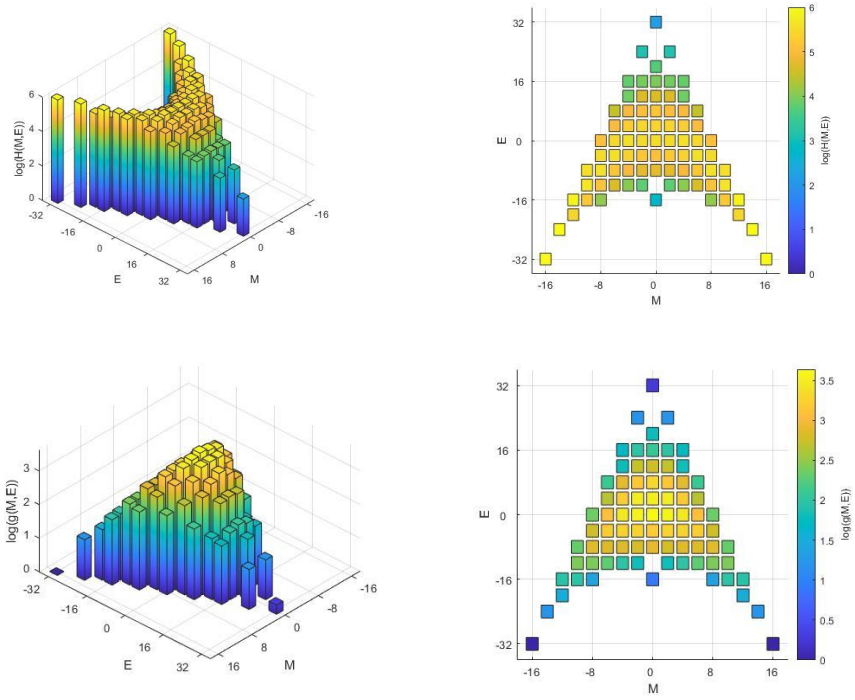

Figure 9 – In the first two figures we observe the logarithm of the histogram from two different angles while the bottom two figures represent the logarithm of the normalized JDoS (L = 4).

The construction of the histogram for L = 4 is shown in sweet.ua.pt/pedromncapelas/RPS14.avi and http://sweet.ua.pt/pedromncapelas/RPS24.avi.

For a system with L = 8 the method does not fully explore the phase space. However, it does a much better job in doing so compared to the Hüller-Pleimling method (figure 10).

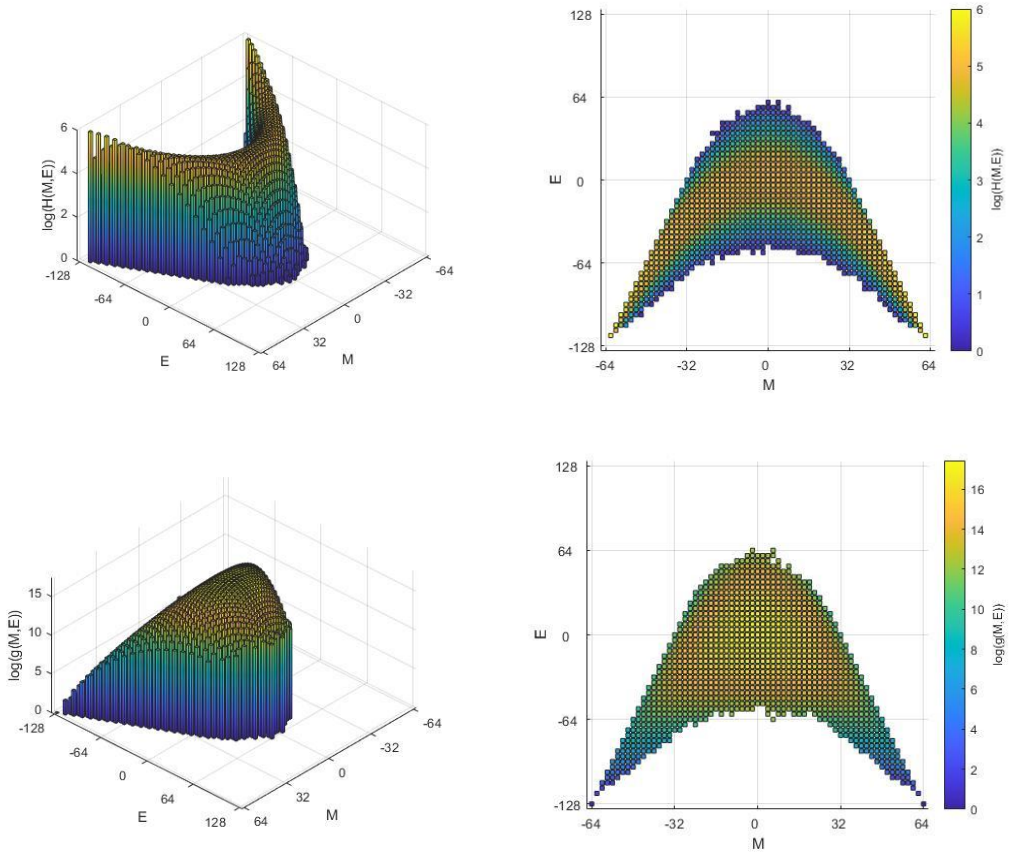

Figure 10 - In the first two figures we observe the logarithm of the incomplete histogram from two different angles while the bottom two figures represent the logarithm of the normalized JDoS (L = 8).

The construction of the histogram for L = 8 is shown in http://sweet.ua.pt/pedromncapelas/RPS18.avi and http://sweet.ua.pt/pedromncapelas/RPS28.avi.

The normalization of the histogram results of considering the limit presented in equation 3.2. For each vector of energies whose value of magnetization is M, we multiply it for the number of possible configurations with magnetization M, $\Omega(M)$.

$$\lim_{R\to\infty} \frac{H(M,E)}{R}\Omega(M) = g(M,E) \tag{3.2}$$

Even if it is not possible to have an infinite number of sweeps, we can approximate the JDoS with the same expression (3.3):

$$g(M,E) \approx \frac{H(M,E)}{R}\Omega(M). \tag{3.3}$$

To determine $\Omega(M)$ we must calculate what configurations with a number of up $N_\uparrow$ and down spins $N_\downarrow$ have a certain value of magnetization [7]. With the help of statistics and combinations we can write this value as being

$$\Omega(M) = \binom{N}{N_\downarrow} = \frac{N!}{N_\downarrow!\,(N-N_\downarrow)!}\,, \tag{3.4}$$

$$N_\downarrow = \frac{N-M}{2}. \tag{3.5}$$

The grey boxes presented contain a sample of pseudocode whose purpose is to calculate the JDoS using the RPS method.

```
Define constants like the size of the system and the number of
nearest neighbours
Calculate energy list
Calculate magnetization list
Nearest neighbours calculation
```

In the beginning of the code, constants like the size of the system, the number of sweeps and the energy and magnetization vectors are defined. The neighbour tables are defined using the aforementioned function “function_NN_list_2D_SS”.

```
Histogram = 0
for number of repetitions
    Define spin vector as being in the all up configuration
    Define randomly the order in which the spins will flip
    Energy calculation (for all up configuration)
    for every value of magnetization (except the first value)
        Spin flip
        New energy calculation
        New magnetization calculation
        Histogram update
    end for
end for
```

Following this, the histogram matrix is defined, and the method is introduced in the "for" loop. In the first place, a spin vector of up spins is created, (the first configuration: all up), its energy is calculated and a random permutation of length L^2 is created (allowing the method to flip a random spin until every spin is flipped down). The second loop is responsible for flipping the spins according to the random permutation, calculating the magnetization and local energy update values, and adding a value to the histogram for each energy and magnetization pair visited.

```
for every magnetization value
     JDOS(M) = Histogram(M) * normalization_factor(M)/Repetitions
end for
```

The normalization is done using the expression shown in 3.3 where the normalization factor is calculated through the expression given in 3.4.

3.4 Wang-Landau Method

The Wang-Landau method, introduced in 2001, results of the observation that a random walk through phase space with probability proportional to the reciprocal of the Joint Density of States should result in a flat histogram [12]. Even though this method has been used as an empirical method, it is one of the most used methods in the calculation of the JDoS due to its capability of not getting stuck in local energy and magnetization minima [8][13].

The idea behind this algorithm is to do a random walk through phase space by flipping spins randomly while only accepting spin flips with a probability proportional to the reciprocal of the JDoS. The problem with this premise is that we do not have the JDoS *à priori*. The algorithm tries to solve this by constructing it while the random walk is being done. However, this results in the accumulation of statistical error in the beginning of the random walk that, later, ends up making the method less exact. A new problem arises: although the Wang-Landau is better than the other methods studied at visiting every possible microstate and creating a complete JDoS, the value to which it converges is not the true value [13].

The algorithm is as follows: We define $g(M,E) = 1$ for every possible magnetization-energy pair as a starting guess. A spin is randomly chosen, and a spin flip is tried. After both the magnetization and energy are calculated for the starting and ending microstates, we establish a criterion by which we will accept or reject this spin flip. This criterion is given by

$$p(M_1, E_1 \rightarrow M_2, E_2) = \min\left[1, \frac{g(M_1, E_1)}{g(M_2, E_2)}\right] \tag{3.6}$$

where E_1, E_2, M_1 and M_2 are the energies and magnetizations before and after the spin flip and $p(M_1, E_1 \rightarrow M_2, E_2)$ is the probability of this spin flip being accepted. By analysing this expression, we can realize that, if $g(M_1, E_1) > g(M_2, E_2)$ the spin flip will always be accepted. If the opposite occurs, the probability will be given by $g(M_1, E_1)/\, g(M_2, E_2)$.

After the criterion is created, a modification factor f is defined so that, if a spin flip is accepted:

$$g(M_2, E_2) = \; g(M_2, E_2) \times f. \tag{3.7}$$

The modification factor can take a range of values, but the standard value to use is Euler's number e. If this value is too small, the time required to visit every possible microstate will be larger. On the other hand, if this value is too big, the accumulation of statistical error will be larger.

On the practical side, these values get big, rendering the expressions 3.6 and 3.7 almost impossible to use. To get around this problem, we apply the natural logarithm to these expressions becoming

$$p(M_1, E_1 \rightarrow M_2, E_2) = \min\{1, \exp\left(\ln[g(M_2, E_2)] - \ln[g(M_2, E_2)]\right\}, \quad (3.8)$$

$$\ln[g(M_2, E_2)] = \ln[g(M_2, E_2)] + \ln(f), \quad (3.9)$$

respectively.

Following this, we update the histogram in the same fashion as the previous methods:

$$H(M_2, E_2) = H(M_2, E_2) + 1. \quad (3.10)$$

The random walk is then continued until a condition of flatness is met. This condition is normally given by a percentage of flatness so that

$$\min[H(M, E)] > a \times \text{mean}[H(M, E)] \cap \max[H(M, E)] < (2 - a) \times \text{mean}[H(M, E)], \quad (3.11)$$

where a is a value between 0 and 1.

After this, in the end of the algorithm, we define a new value of f so that

$$f_{n+1} = \sqrt{f_n}. \quad (3.12)$$

Finally, after every step, we reset the histogram matrix to 0 while keeping the JDoS estimate intact, and we repeat everything until f reaches a defined value.

We can observe two flat histograms in figure 11 for L = 4 and L = 8, respectively.

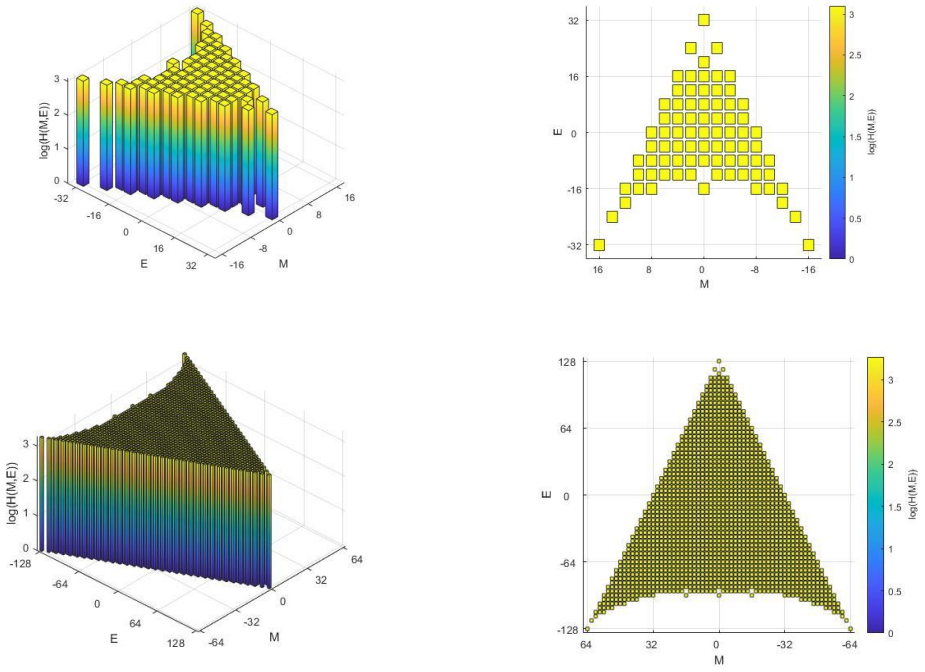

Figure 11 - The first two figures represent the logarithm of the histogram for L = 4 from two different angles while the bottom two figures represent the logarithm of the histogram for L = 8.

The normalization can be done in two different ways:

1. Knowing the value of the JDoS for a certain magnetization-energy pair, i.e. we know that the number of ground states (E = -2N) is 2.

2. We consider that the total number of states is given by

$$\sum_{E} g(E) = 2^{N} . \tag{3.13}$$

The first way guarantees the exactness of the JDoS for low values of temperature, which is good if we want to calculate thermodynamic properties at low temperatures. In the second one the rescaling factor is influenced by the maximum JDoS, making the low temperature values inaccurate. We can utilize one of the two methods to calculate the density of states and the other one to check the accuracy of our results [14].

Observing how the JDoS is calculated reveals that the "walker" does not follow the same rules dependent of the Wang-Landau cycle. A system with L = 4 is too small to observe

what is really happening so we will be using L = 8 to observe how the different histograms of the different Wang-Landau cycles are flattened.

Figures 12 and 13 show 3 frames of the histogram while it is being built for the first and tenth Wang-Landau cycles, respectively.

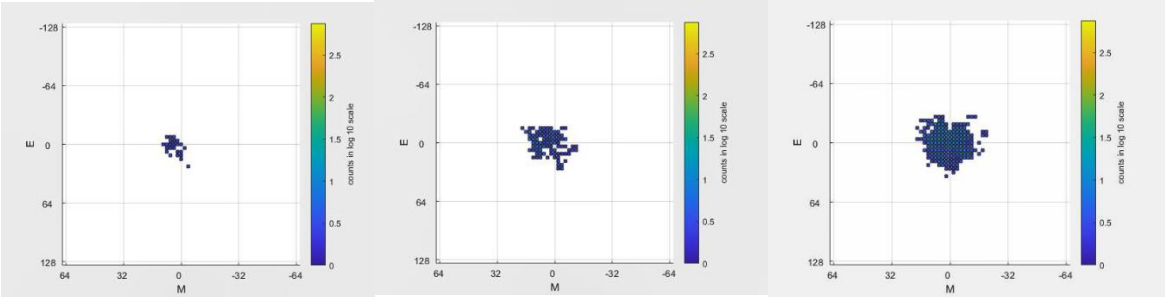

Figure 12 – Representation of three frames from the first Wang-Landau cycle where the sample seems to follow a random walker with no bias or criteria. This video can be watched at http://sweet.ua.pt/pedromncapelas/WL181.avi and http://sweet.ua.pt/pedromncapelas/WL281.avi. Note that the energy values are flipped.

We can clearly observe, in the first cycle, that the "walker" seems to be searching the phase space analogously to a random walker with no bias or criteria, where most of the visited microstates are located at the middle. Compared to this, the "walker" in the tenth cycle demonstrates a completely different behaviour. It seems to visit the less visited states in defined pathways.

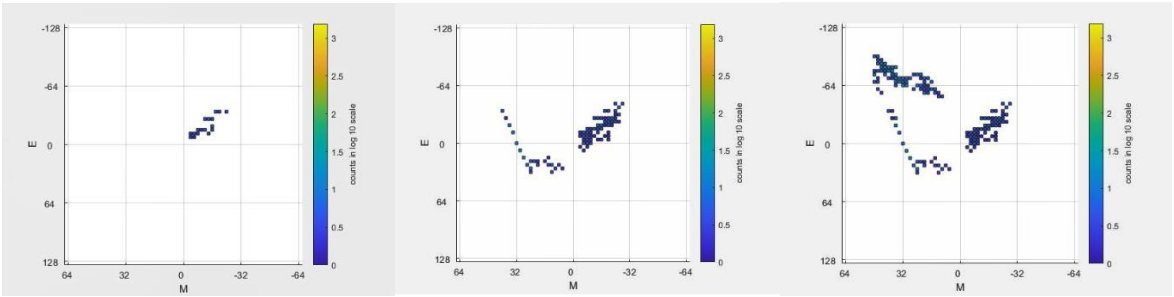

Figure 13 - Representation of three frames from the tenth Wang-Landau cycle where the sample seems to follow specific pathways, a radically different behavior from the first cycle. This video can be watched at http://sweet.ua.pt/pedromncapelas/WL182.avi and http://sweet.ua.pt/pedromncapelas/WL282.avi. Note that the energy values are flipped.

One defining difference between the first and tenth cycles is the value of the modification factor. For the first cycle this factor is defined as being $f_0 = e$ and, for the tenth cycle, $f_9 \approx 1.057$. If we apply the natural logarithm to these (to apply the expression 3.9) we quickly realise that the change created in the JDoS by a microstate being visited in the

first cycle is much greater than if it was visited in the tenth cycle. We can conclude that, in the Wang-Landau method, the bulk of the JDoS is calculated on the first cycles while the last cycles serve the purpose of refining it.

A sample of pseudocode is presented in the grey box where E_o and M_o denominate the energy and magnetization of the old configuration while E_n and M_n denominate the energy and magnetization of the new configuration.

```
while f is bigger than some value we define
      Histogram = 0
      while histogram is not flat
            Original Configuration
            Random Spin Flip
            E and M calculation
            if spin flip is accepted (by the criterion)
                  ln(JDoS(M_n,E_n)) = ln(JDoS(M_n,E_n)) + ln(f)
                  Histogram(M_n,E_n) = Histogram(M_n,E_n) + 1
                  M_o = M_n
                  E_o = E_n
            end if
            else
                  Spin flip is rejected
                  ln(JDoS(M_o,E_o)) = ln(JDoS(M_o,E_o)) + ln(f)
                  Histogram(M_o,E_o) = Histogram(M_o,E_o) + 1
            end else

      end while
end while
```

The final JDoS for L = 4 (with 17 Wang-Landau cycles) and L = 8 (with 10 Wang-Landau cycles) is shown in figure 14.

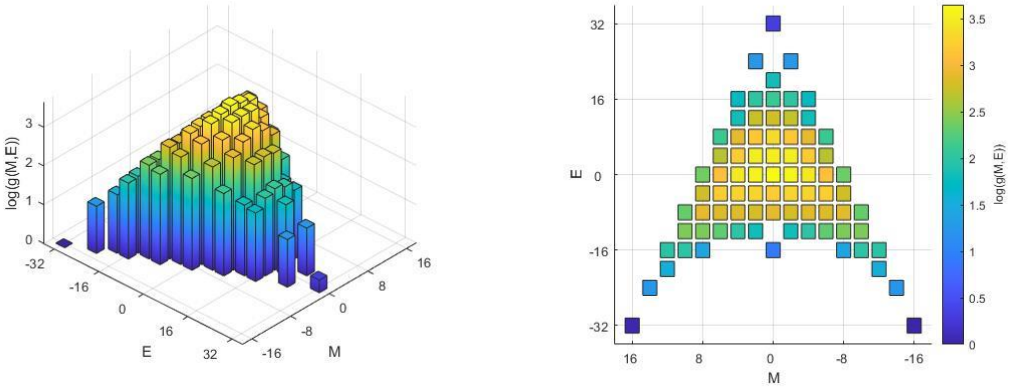

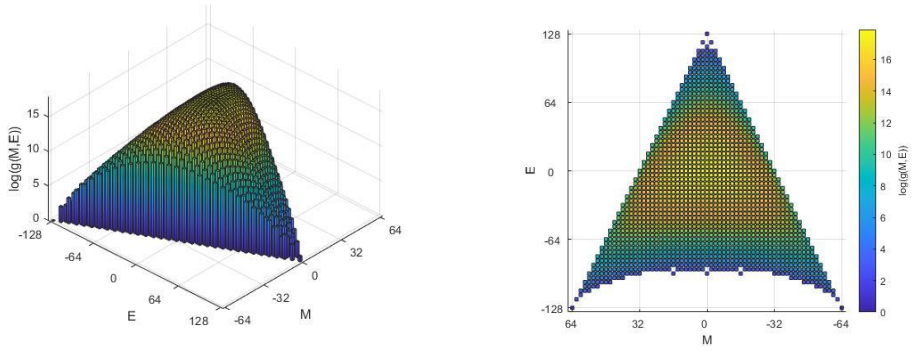

Figure 14 - In the first two figures we observe the logarithm of the normalized JDoS (L = 4) from two different angles while the bottom two figures represent the logarithm of the normalized JDoS (L = 8).

To observe how the histogram for L = 4 is built for the first Wang-Landau cycle: http://sweet.ua.pt/pedromncapelas/WL141.avi and http://sweet.ua.pt/pedromncapelas/WL241.avi. For the second cycle: http://sweet.ua.pt/pedromncapelas/WL142.avi. and http://sweet.ua.pt/pedromncapelas/WL242.avi.

Chapter 4

Conclusion and future work

4.1 Conclusion

In this work three different methods were presented: the Hüller-Pleimling method, Random Path Sampling and, lastly, the Wang-Landau method.

For a square-lattice Ising model with L = 4, every method (including the unbiased random sampling) calculated a complete JDoS as we can see in figure 15.

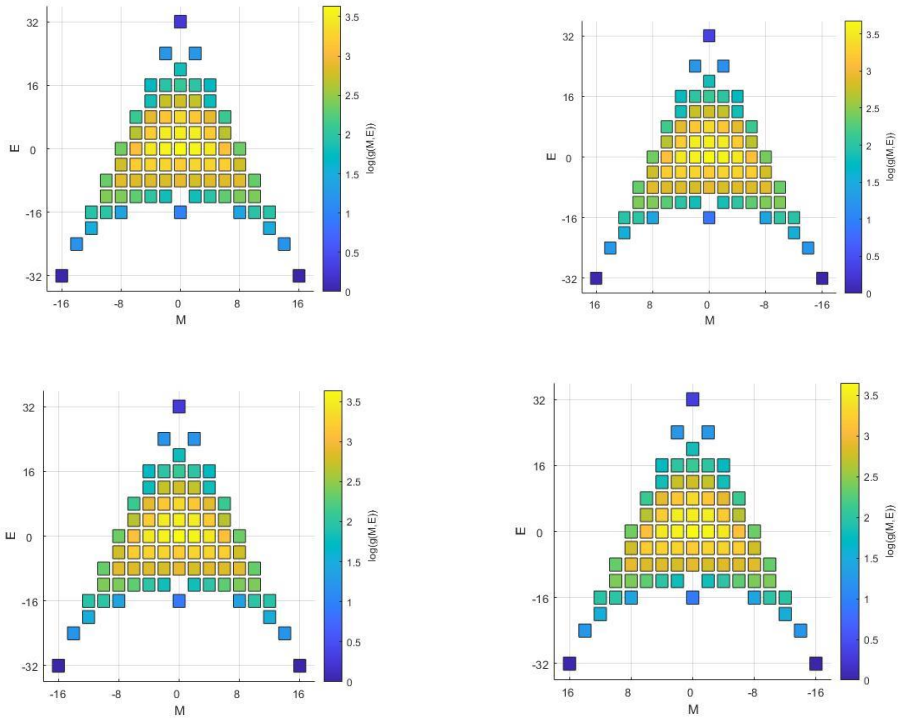

Figure 15 – Comparison between JDoS estimates from the various methods here explored for L=4. Top left: unbiased random sampling ; Top right: Hüller-Pleimling method; Bottom left: RPS and bottom right: Wang-Landau method.

As we can see, every result is almost indistinguishable from each other and, for comparison, the relative error for every method will be calculated since we have access to

the exact JDoS for L = 4. The relative error is given by expression 4.1 where $g^*(M,E)$ is the approximate JDoS calculated by the method and $g(M,E)$ is the exact JDoS.

$$E_{relative} = \sum_{M,E} \frac{|g^*(M,E) - g(M,E)|}{g(M,E)} \tag{4.1}$$

The relative error is presented in the table 2.

Table 2 – Relative error for random sampling and the three studied methods, compared to the exact JDoS. These result of the average between ten runs of each method.

Method	$\overline{E_{relative}}$
Random Sampling	12.3
Hüller-Pleimling	9.3
Random Path Sampling	0.34
Wang-Landau	0.5

Every method was tested with the conditions explained in chapter 3. Comparing the computing times, the first three methods were similar. However, the Wang-Landau method took around two times longer to complete, highlighting the RPS method since it was the best of the four. For bigger systems (like L = 8) we see the Wang-Landau method standing out in comparison (figure 16).

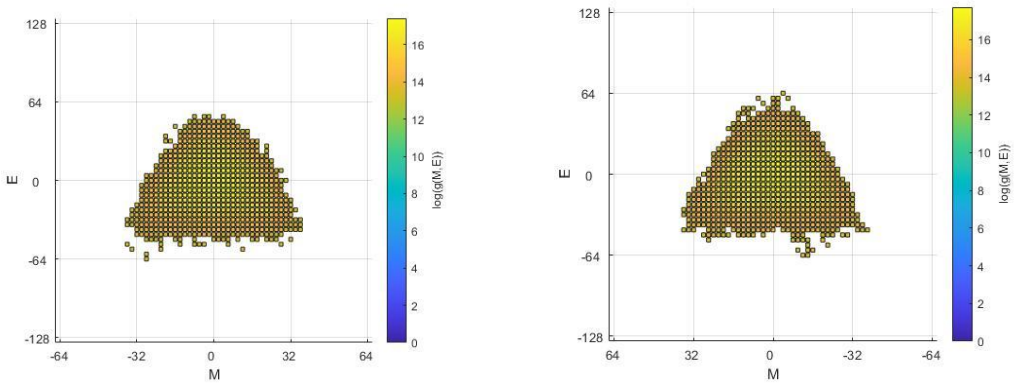

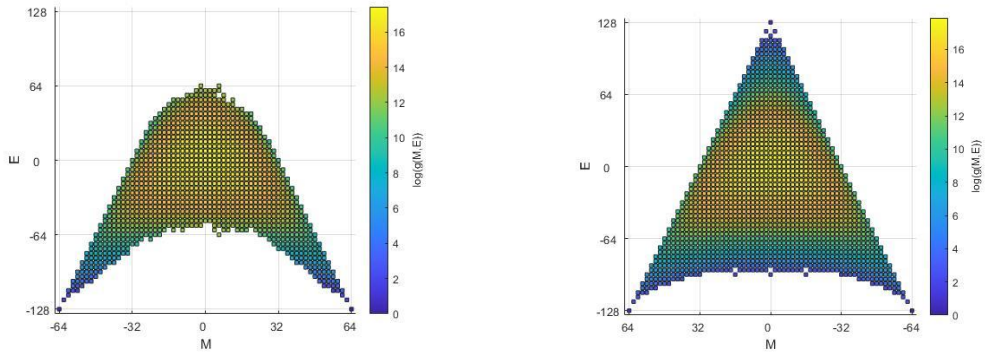

Figure 16 – Comparison between JdoS estimates from the various methods here explored for L=8. Top left: unbiased random sampling; Top right: Hüller-Pleimling method; Bottom left: RPS and bottom right: Wang-Landau method.

Both the random sampling and the Hüller-Pleimling method were very similar, only visiting the most probable microstates. On the other hand, the RPS method searched the phase-space much better in comparison, visiting a considerable amount of magnetization-energy pairs present in the branch that connects the all up/down states with the middle of the phase-space. Finally, the Wang-Landau method is the only one that visits every possible magnetization-energy pair, creating a complete JDoS. However, to achieve this, this method took around 3 times more computing time in comparison to the other methods. To highlight the difference between the RPS and Wang-Landau methods, figure 17 shows the density of states for M = 0 where we clearly see that the missing microstates are located on the energy extremes.

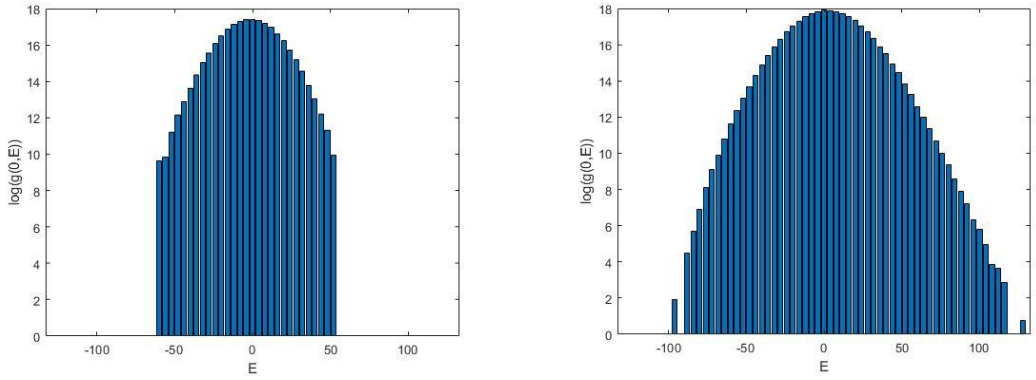

Figure 17 – The figure in the left represents de density of states for L = 8 and M = 0 created by the RPS method while the figure in the right represents the same density of states but created using the Wang-Landau method.

An important question arises: if we use the same computing time for every method would the first three methods get a much better result in comparison with the Wang-Landau method? To answer this question, let us only consider the RPS method (since it is the best of the first three methods) and the density of states for M = 0 presented in figure 17.

The least probable magnetization-energy pair to visit (for M = 0) is that with the highest energy, also known as the checkerboard state (since is resembles a checkerboard where the black and white squares represent opposing spins). There are 2 microstates that have this energy and, therefore, the probability of visiting one of them is given by the expression 4.2,

$$p = \frac{2}{\Omega(0)}\ , \tag{4.2}$$

where $\Omega(0)$ is the number of microstates that have M = 0. This way, on average, the number of repetitions we would need to visit this specific energy value is given by the reciprocal of the probability:

$$REP = \frac{\Omega(0)}{2} \approx 9.163 \times 10^{17}\ . \tag{4.3}$$

We can conclude that, if we equalized the computing time of the RPS with that of the Wang-Landau method, we would not observe much improvement since we would need the RPS time to be orders of magnitude larger to ever visit some of the least probable microstates.

4.2 Future work

This work focuses completely on estimating the Joint Density of States (JDoS) of the 2D Ising model by different Monte-Carlo methods. However, there are many more things that can be done to further this to computational materials design. The next logical step is to calculate the thermodynamic properties of the Ising model, like the partition function and Helmholtz free energy, with the objective of calculating the equilibrium behaviour of this model in finite temperature.

As previously said, although the Ising model can provide a well-defined phase transition, it does not represent a real material. We could study different models beside the Ising model, like the Heisenberg model, that is much more useful in representing how real ferromagnets work, due to its increased degrees of freedom.

One important aspect that should be studied is on how to increase the efficiency of the methods studied and the use of vectorization and parallelization to decrease computation time [15].

This work was made exclusively in MATLAB since its interface is one of best to understand and visualize how these methods work. However, the efficiency of this programming language falls short in comparison to other programming languages like C and should be avoided for intensive workloads (C has been seen having wall times 80 times lower than MATLAB [7]). For this reason, one future work could be to implement these methods in other, more efficient languages.

The study of the three-dimensional Ising model is of great interest since it has no analytic solution and could be approached in future work [16].

In this work we studied three different methods to calculate the JDoS of the Ising Model. However, new and better (and also much more complicated to implement) versions of these methods have been published in the years following their introduction and their study is a subject to consider in future work.

Chapter 5

References

[1] S. Blundell, “Magnetism in Condensed Matter,” *OXFORD Univ. Press*, 2001, doi: 10.1017/CBO9781107415324.004.

[2] J. C. S. Amaral, “Estudo de Manganites Modificadas com Iões de Terra Rara,” Universidade de Aveiro, 2005.

[3] S. Sanvito *et al.*, “Accelerated discovery of new magnets in the Heusler alloy family,” *Sci. Adv.*, 2017, doi: 10.1126/sciadv.1602241.

[4] S. Curtarolo, G. L. W. Hart, M. B. Nardelli, N. Mingo, S. Sanvito, and O. Levy, “The high-throughput highway to computational materials design,” *Nat. Mater.*, 2013, doi: 10.1038/nmat3568.

[5] W. Chen, J. George, J. B. Varley, G. M. Rignanese, and G. Hautier, “High-throughput computational discovery of In2Mn2O7 as a high Curie temperature ferromagnetic semiconductor for spintronics,” *npj Comput. Mater.*, vol. 5, no. 1, 2019, doi: 10.1038/s41524-019-0208-x.

[6] W. P. Wolf, “The Ising model and real magnetic materials,” *Brazilian Journal of Physics*. 2000, doi: 10.1590/S0103-97332000000400030.

[7] N. Fortunato, “Amostragem Por Caminho Aleatório Aplicado a Modelos Vetoriais de Magnetismo,” Universidade de Aveiro, 2015.

[8] C. Zhou, T. C. Schulthess, S. Torbrügge, and D. P. Landau, “Wang-landau algorithm for continuous models and joint density of states,” *Phys. Rev. Lett.*, vol. 96, no. 12, pp. 8–11, 2006, doi: 10.1103/PhysRevLett.96.120201.

[9] D. P. Landau and K. Binder, *A Guide to Monte Carlo Simulations in Statistical Physics*. 2005.

[10] A. Hüller and M. Pleimling, “Microcanonical determination of the order parameter critical exponent,” *Int. J. Mod. Phys. C*, vol. 13, no. 7, pp. 947–956, 2002, doi: 10.1142/S0129183102003693.

[11] J. S. Amaral, J. N. Gonçalves, and V. S. Amaral, “Thermodynamics of the 2-D Ising Model from a Random Path Sampling Method,” *IEEE Trans. Magn.*, vol. 50, no. 11, pp. 2–5, 2014, doi: 10.1109/TMAG.2014.2326713.

[12] F. Wang and D. P. Landau, “Efficient, multiple-range random walk algorithm to calculate the density of states,” *Phys. Rev. Lett.*, vol. 86, no. 10, pp. 2050–2053, 2001, doi: 10.1103/PhysRevLett.86.2050.

[13] C. Zhou and R. N. Bhatt, “Understanding and improving the Wang-Landau algorithm,” *Phys. Rev. E - Stat. Nonlinear, Soft Matter Phys.*, vol. 72, no. 2, pp. 10–13, 2005, doi: 10.1103/PhysRevE.72.025701.

[14] “Density of States of the 2D Ising Model.” http://stp.clarku.edu/simulations/ising/wanglandau/index.html (accessed Jul. 15, 2020).

[15] A. Valentim *et al.*, “Exploring Replica-Exchange Wang-Landau sampling in higher-dimensional parameter space,” *J. Phys. Conf. Ser.*, vol. 640, no. 1, 2015, doi: 10.1088/1742-6596/640/1/012006.

[16] A. M. Ferrenberg, J. Xu, and D. P. Landau, “Pushing the limits of Monte Carlo simulations for the three-dimensional Ising model,” *Phys. Rev. E*, vol. 97, no. 4, p. 43301, 2018, doi: 10.1103/PhysRevE.97.043301.